Available online at www.sciencedirect.com

SCIENCE DIRECT

Biochimica et Biophysica Acta 1668 (2005) 248–261

BIOCHIMICA ET BIOPHYSICA ACTA BBA

http://www.elsevier.com/locate/bba

Nucleotide dissociation from NBD1 promotes solute transport by MRP1☆

Runying Yang, Ali McBride, Yue-xian Hou, Aaron Goldberg, Xiu-bao Chang*

Mayo Clinic College of Medicine, Mayo Clinic, Scottsdale, AZ 85259, USA

Received 28 September 2004; received in revised form 28 December 2004; accepted 28 December 2004
Available online 2 February 2005

Abstract

MRP1 transports glutathione-S-conjugated solutes in an ATP-dependent manner by utilizing its two NBDs to bind and hydrolyze ATP. We have found that ATP binding to NBD1 plays a regulatory role whereas ATP hydrolysis at NBD2 plays a dominant role in ATP-dependent LTC4 transport. However, whether ATP hydrolysis at NBD1 is required for the transport was not clear. We now report that ATP hydrolysis at NBD1 may not be essential for transport, but that the dissociation of the NBD1-bound nucleotide facilitates ATP-dependent LTC4 transport. These conclusions are supported by the following results. The substitution of the putative catalytic E1455 with a non-acidic residue in NBD2 greatly decreases the ATPase activity of NBD2 and the ATP-dependent LTC4 transport, indicating that E1455 participates in ATP hydrolysis. The mutation of the corresponding D793 residue in NBD1 to a different acidic residue has little effect on ATP-dependent LTC4 transport. The replacement of D793 with a non-acidic residue, such as D793L or D793N, increases the rate of ATP-dependent LTC4 transport. Along with their higher transport activities, their Michaelis constant K_ms (ATP) are also higher than that of wild-type. Coincident with their higher K_ms (ATP), their K_ds derived from ATP binding are also higher than that of wild-type, implying that the rate of dissociation of the bound nucleotide from the mutated NBD1 is faster than that of wild-type. Therefore, regardless of whether the bound ATP at NBD1 is hydrolyzed or not, the release of the bound nucleotide from NBD1 may bring the molecule back to its original conformation and facilitate the protein to start a new cycle of ATP-dependent solute transport.

Keywords: Multidrug resistance-associated protein 1; Nucleotide binding domain; ATP binding; Dissociation of the bound ATP; ATP hydrolysis; ATP-dependent LTC4 transport

1. Introduction

The over-expression of either P-glycoprotein (ABCB1 or P-gp), breast cancer resistant protein (ABCG2 or BCRP) and/or multidrug resistance-associated protein 1 (ABCC1 or MRP1) confers cancer cells with resistance to a broad range of anticancer drugs. Although these ATP-binding cassette (ABC) transporters transport anti-cancer drugs out of cells in an ATP-dependent manner by utilizing their membrane-spanning domains and nucleotide binding domains (NBDs) [1–16], the means by which they pump drugs out of cells are different, i.e. for example, P-gp transports hydrophobic compounds directly [1–3], whereas MRP1 transports anionic conjugates, such as glutathione-S-conjugates [4–12]. Therefore it is reasonable to ask whether they share the same mechanism of coupling ATP binding/hydrolysis to anti-cancer drug transport.

In the extensively studied P-gp, its two NBDs have been shown to be functionally equivalent with identical ATP hydrolysis steps occurring alternately at each NBD [17,18]. If one NBD enters the transition-state conformation, the other site is prohibited from doing so [17,19,20]. The mutation of an essential residue in the Walker A motif in either NBD

☆ This work was supported by grant CA89078 from National Cancer Institute, National Institutes of Health.

Abbreviations: P-gp, P-glycoprotein; MRP1, multidrug resistance-associated protein 1; NBD, nucleotide binding domain; LTC4, leukotriene C4; SDS, sodium dodecyl sulfate; EDTA, ethylenediaminetetraacetic acid; 8-N_3ATP, 8-azidoadenosine 5′ -triphosphate; Sf21, *Spodoptera frugiperda* 21

* Corresponding author. S.C. Johnson Medical Research Center, Mayo Clinic Scottsdale, 13400 East Shea Blvd., Scottsdale, AZ 85259, United States. Tel.: +1 480 301 6206; fax: +1 480 301 7017.
E-mail address: xbchang@mayo.edu (X. Chang).

0005-2736/$ - see front matter © 2005 Elsevier B.V. All rights reserved.
doi:10.1016/j.bbamem.2004.12.013

completely abolishes ATP-dependent transport activity [21,22]. Similarly, the covalent modification of either site completely blocks the turnover of ATP [17,23]. Although some reports indicated that the two NBDs of P-gp were essential for its function but not entirely symmetric [24,25], most NBD1 segments could be replaced by homologous segments of NBD2 without a loss of P-gp function [26]. It has been clearly demonstrated that the two NBDs of MRP1 have different properties and functions [27–30]. Thus, P-gp and MRP1 may not share the same mechanism to couple ATP binding/hydrolysis to anti-cancer drug transport.

It has been reported that there are two independent ATP hydrolysis events in a single drug transport cycle by P-gp, one associated with drug transport and the other causing conformational resetting to the original state of the molecule [31,32]. In addition, these two NBD sites, with equal affinity for ATP, are recruited randomly [31,32]. The two ATP binding/hydrolysis sites of MRP1 seem not to be recruited in a random manner because photolabeling by the non-hydrolyzable [α-^{32}P]-8-N_3AMP–PNP occurred predominately at NBD1 in the absence of other nucleotides and was shifted to NBD2 by a low concentration of 8-N_3ATP, implying that NBD1 may have a higher affinity for nucleotide than NBD2 and the binding of 8-N_3ATP at NBD1 induces a conformational change of the molecule and enhances AMP–PNP binding at NBD2 [33]. Indeed, NBD1 of MRP1 has slightly higher affinity for ATP than NBD2 [34]. A similar conclusion can also be reached from experiments in which the N-proximal half and C-proximal half of MRP1 are expressed simultaneously in Sf21 cells and labeled with either [α-^{32}P]-8-N_3ATP or [γ-^{32}P]-8-N_3ATP on ice [27]. It is also clear that the two NBDs of other ABC proteins, including the sulfonylurea receptor (ABCC8 or SUR1) [35] and cystic fibrosis transmembrane conductance regulator (ABCC7 or CFTR) [36–38], have very distinctive properties.

The functioning of the acidic amino acid directly adjacent to the aspartic acid in Walker B motif as a catalytic

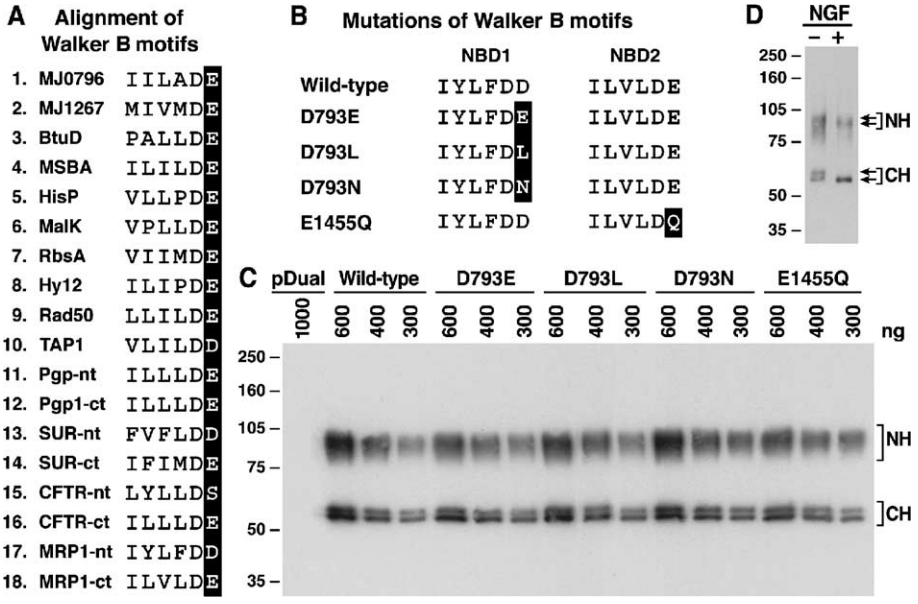

Fig. 1. Expression of wild-type and putative catalytic base mutant MRP1s in Sf21 insect cells. (A) Sequence alignment of Walker B motifs, including the acidic amino acid directly adjacent to the highly conserved D residue in Walker B motif, from some of the ABC transporters. The highlighted letters indicate the putative catalytic base interacting with the water molecule [39,40]. The terms nt and ct indicate N-proximal (NBD1) and C-proximal (NBD2) Walker B motifs. (B) Mutations of the putative catalytic bases in human MRP1 protein. The highlighted letters indicate the D to E, L and N mutations in NBD1 and E to Q mutation in NBD2. The definition of D793E means that the D793E mutated N-half is co-expressed with wild-type C-half and E1455Q, the wild-type N-half co-expressed with E1455Q mutated C-half. (C) Expression of wild-type and mutant variants of human MRP1 protein in Sf21 cells. Membrane vesicles were prepared from Sf21 cells infected with viral particles expressing pDual without MRP1 cDNA insertion (lane 1), wild-type N-half+wild-type C-half (Wild-type, lanes 2–4), D793E mutated N-half+wild-type C-half (D793E, lanes 5–7), D793L mutated N-half+wild-type C-half (D793L, lanes 8–10), D793N mutated N-half+wild-type C-half (D793N, lanes 11–13) and wild-type N-half+E1455Q mutated C-half (E1455Q, lanes 14–16). The amounts (ng) of membrane vesicle proteins loaded in the gel are indicated on top of the gel. The membrane proteins were resolved on a 7% SDS-PAGE, electroblotted to a nitrocellulose membrane and probed with MRP1-specific mAb 42.4 and 897.2 [28,29]. The molecular weight markers are indicated on the left. NH and CH on the right indicated the N-proximal half and C-proximal half of the MRP1 proteins. The intensities of the N-half and C-half bands were measured by a scanning densitometer. The ratios of the band intensities in the same amount of total membrane proteins, for example, 300 ng of wild-type N-half (co-expressed with wild-type C-half) versus 300 ng of the D793E mutated N-half (co-expressed with wild-type C-half), were determined, considering the amount of wild-type N-half (or C-half) as 1.000. Since the ratio of N-half, for example, D793E mutated N-half, is similar to that of the C-half co-expressed with D793E mutated N-half, the mean ratios of the protein expressions including N-half and C-half are: 0.993±0.168 (D793E), 0.991±0.073 (D793L), 1.151±0.186 (D793N) and 0.921±0.108 (E1455Q). (D) The lower mobility band of C-half is glycosylated whereas the higher mobility band of C-half is not. Membrane vesicles containing wild-type N-half and C-half were incubated in the absence (−) or presence (+) of *N*-glycosidase F and resolved (500 ng) on a 7% SDS-PAGE. The upper arrow in NH or CH indicates the glycosylated N-half or C-half, whereas the lower arrow in NH or CH indicates the de-glycosylated (or un-glycosylated) N-half or C-half.

base during ATP hydrolysis [39,40] provides another tool to analyze the function of each NBD. As shown in Fig. 1A most ABC transporters have a Glu residue at this position, except TAP1, NBD1 of SUR1 and MRP1 which have an Asp and NBD1 of CFTR, a Ser residue. The mutation of this catalytic residue in bacterial ABC transporter MJ0796 or MJ1267 [41] or HisP [39] produced proteins that bind nucleotide normally, but cannot efficiently hydrolyze ATP. Interestingly, the mutation of this putative catalytic residue in either NBD1 or NBD2 of P-gp resulted in a loss of ATPase activity, however, drugs can still stimulate vanadate-dependent trapping of ADP at a level similar to that of wild-type P-gp [42], implying that ATP hydrolysis still occurs but that release of ADP is impaired. These results indicated that the release of the bound nucleotide is also important for the proper function of an ABC transporter. Counterpart mutations in NBD1 and NBD2 of MRP1 have different effects on ATP-dependent LTC4 transport. The mutation of this putative catalytic Glu residue in the NBD2 of MRP1 to a negatively charged Asp with a shorter side chain completely eliminates ATP-dependent LTC4 transport activity [43]. In contrast, an Asp to Glu change in the NBD1 of MRP1 retains a certain level of ATP-dependent LTC4 transport activity [43], whereas the mutation of the same residue to a non-acidic Leu residue enhances the ATP-dependent LTC4 transport activity [29]. To investigate the roles played by the NBD1 of MRP1 during ATP-dependent solute transport, we have mutated the putative catalytic base D793 in NBD1 to E, L and N and E1455 in NBD2 to Q (Fig. 1B). This mutation in NBD2 (E1455Q) almost completely eliminates ATP-dependent LTC4 transport. In contrast, the mutation of the putative catalytic residue D793 to a non-acidic amino acid, such as Asn, increases the dissociation rate of the bound nucleotide from NBD1 and the rate of ATP-dependent LTC4 transport. These results are interpreted as indicating that ATP hydrolysis at NBD2 is directly coupled to an ATP-dependent solute transport, whereas the release of the NBD1-bound nucleotide may return the molecule to its original conformation so that the protein can start a new cycle of ATP-dependent solute transport.

2. Materials and methods

2.1. Materials

EDTA, ATP and ouabain were purchased from Sigma. [α-^{32}P]-8-N_3ATP, [α-^{32}P]-8-N_3AMP–PNP and [γ-^{32}P]-8-N_3ATP were purchased from AFFINITY LABELING TECHNOLOGIES. [14,15,19,20-^{3}H]leukotriene C4 was from NEN life Science Products. Grace's insect cell culture medium was from Invitrogen. Fetal bovine serum was from Gemini Bio-Products. The Stratalinker UV Crosslinker 2400 model (wavelength 254 nm) and QuikChange site-directed mutagenesis kit were from Stratagene. Chemiluminescent substrates were from Pierce.

2.2. Cell culture and expression of MRP1s

Spodoptera frugiperda 21 (Sf21) cells were cultured in Grace's insect cell medium supplemented with heat-inactivated 5% fetal bovine serum at 27 °C. Viral infection was performed according to Invitrogen's recommendation.

2.3. Generation of constructs

The oligo-nucleotides to introduce the mutations in MRP1 are: MRP/D793E/forward, 5′-CT GAC ATT TAC CTC TTC GAT GAA CCC CTC TCA GCA GTG GAT GCC-3′; MRP/D793E/reverse, 5′-GGC ATC CAC TGC TGA GAG GGG TTC ATC GAA GAG GTA AAT GTC AG-3′; MRP/D793N/forward, 5′-CT GAC ATT TAC CTC TTC GAT AAT CCC CTC TCA GCA GTG GAT GCC -3′; MRP/D793N/reverse, 5′-GGC ATC CAC TGC TGA GAG GGG ATT ATC GAA GAG GTA AAT GTC AG-3′; MRP/E1455Q/forward, 5′-G AAG ATC CTT GTG TTG GAT CAG GCC ACG GCA GCC GTG GAC CTG G-3′; MRP/E1455Q/reverse, 5′-C CAG GTC CAC GGC TGC CGT GGC CTG ATC CAA CAC AAG GAT CTT C-3′. The underlined sequences are mutated nucleotides. The coding sequence of human MRP1 cDNA in the pNUT expression vector [44] was used as a template for the mutagenesis. The aspartic acid residue at position 793 was mutated to either glutamic acid or asparagine (Fig. 1B, D793E or D793N) by using the forward/reverse primers and the QuikChange site directed mutagenesis kit from Stratagene [28]. D793L was introduced into the cDNA in the pNUT expression vector already [29]. E1455Q was also introduced into the cDNA by the same strategy. To clone the N-proximal half of MRP1 (from 1 to 932) into pDual (pFASTBACKDUAL from Invitrogen), a piece of DNA fragment, from 1921 to 2992, was amplified by using the forward primer 5′-GAT CGG ACA GAG ATT GGC GAG AAG G-3′ and reverse primer 5′-CTA TGC GGT GCT GTT GTG GTG CCT GCT-3′ containing a stop codon. This amplified fragment was cloned into pBluescript and sequenced completely. The *Eco*RI (from pcDNA3)–*Xho*I (2766) fragment containing 197 to 2766 of wild-type MRP1 cDNA (from pcDNA3/MRP1/His) and the *Xho*I (2766)–*Xba*I (from pBluescript) fragment containing 2767 to 2992 and a stop codon TAG were cloned into pDual vector, named as pDual/N-half (using pPolh promotor). To clone the C-proximal half of MRP1 (from 933 to 1531) into pDual, a piece of DNA fragment, from 2993 to 4093, was amplified by using the forward primer 5′-C GAT ATC ACC ATG GAA CTG CAG AAA GCT GAG GCC AAG-3′ containing a Kozak sequence [45] ACCATGG with an initiation ATG codon and reverse primer 5′-GCA GTA GTT CCG GAA TTC CAC TCG-3′. This amplified fragment was cloned into pBluescript and sequenced completely. The *Eco*RV (from pBluescript)–*Eco*RI (4076) fragment containing extra-sequences CGATATCACCATG (a start codon) and 2993–4076 and the *Eco*RI (4076)–*Kpn*I (from pBluescript)

fragment containing 4076–4789, 10 His codons and a stop codon at the 3′ end were cloned into pDual vector, named as pDual/C-half (using p10 promotor). To make a construct expressing N-half and C-half simultaneously, the *Rsr*II–*Kpn*I fragment containing wild-type C-half was derived from pDual/C-half and cloned into *Rsr*II and *Kpn*I sites of pDual/N-half, named as pDual/N-half/C-half. This strategy was also used to generate constructs expressing D793E, L, and N mutated N-half and E1455Q mutated C-half. To make constructs expressing D793E, D793L and D793N mutated N-half and wild-type C-half simultaneously, the *Kpn*I–*Dra*III fragment from pDual/N-half/C-half and the *Dra*III–*Xho*I fragments from pNUT/D793E, pNUT/D793L or pNUT/D793N were cloned into the *Kip*I–*Xho*I fragment from pDual/N-half/C-half, named as pDual/D793E-N-half/C-half, pDual/D793L-N-half/C-half or pDual/D793N-N-half/C-half. To make a construct expressing wild-type N-half and E1455Q mutated C-half simultaneously, the *Cla*I–*Bsp*EI fragment derived from pNUT/E1455Q and the *Rsr*II–*Cla*I fragment from pDual/N-half/C-half were cloned into the *Rsr*II–*Bsp*EI fragment derived from pDual/N-half/C-half, named as pDual/N-half/E1455Q-C-half.

2.4. Recombinant viral DNA preparation and viral particle production

The generation of recombinant viral DNA was performed according to Invitrogen's recommendation. pDual/MRP1 donor plasmid DNA was transformed into DH10Bac competent cells harboring the parent bacmid with a mini-attTn7 target site and the helper plasmid. Bacteria transformed with the donor plasmid DNA were selected on LB plates containing 50 μg/ml kanamycin, 7 μg/ml gentamicin and 10 μg/ml tetracycline. In addition, colonies containing recombinant bacmids were identified by the disruption of the lacZα gene (white colonies) on the LB plates containing 100 μg/ml 5-bromo-4-chloro-indolyl-β-D-galactoside (X-gal) and 40 μg/ml isopropylthio-β-D-galactoside (IPTG). Single colonies confirmed as having a white phenotype on the LB plates with X-gal and IPTG were inoculated to a medium containing 50 μg/ml kanamycin, 7 μg/ml gentamicin and 10 μg/ml tetracycline. The purified recombinant bacmids were confirmed by polymerase chain reaction with MRP1 specific primers and then used to transfect Sf21 cells with CellFECTIN reagent (Invitrogen). After 3–4 days incubation at 27 °C, the supernatants containing viral particles were collected and the cell lysates (with 2% SDS) were used to do Western blot, probed with MRP1 specific monoclonal antibodies 42.4 and 897.2 [28].

2.5. Viral plaque assay, viral infection and membrane vesicle preparation

Viral plaque assay was performed according to Invitrogen's recommendation. The expression levels of the recombinant proteins with varying multiplicity of infections (MOI) were determined by Western blot, using antibodies 42.4 against NBD1 and 897.2 against NBD2. The MOIs produced similar amounts of N-halves (comparing N-halves only) and C-halves (comparing C-halves only) were used to infect Sf21 cells for membrane vesicle preparations.

MRP1-containing membrane vesicles were prepared according to the procedure described previously [28]. The membrane vesicles were resuspended in an ice-cold solution containing 10 mM Tris–HCl, pH 7.5, 250 mM sucrose and 1×protease inhibitors (2 μg/ml aprotinine, 121 μg/ml benzamidine, 3.5 μg/ml E64, 1 μg/ml leupeptin and 50 μg/ml Pefabloc). After passage through a Liposofast™ vesicle extruder (1000 nm nitrocellulose filter, Avestin, Ottawa, Canada) the membrane vesicles were aliquoted and stored in −80 °C.

2.6. SDS-PAGE and Western blot

SDS-PAGE and Western blot were performed as described previously [28,29]. The primary antibodies used were mouse anti-human MRP1 monoclonal antibodies 42.4 and 897.2 [28,29] and the secondary antibody was anti-mouse Ig conjugated with horseradish peroxidase. Chemiluminescent film detection was performed according to the manufacturer's recommendations (Pierce).

To remove N-linked oligosaccharides by cleavage of the asparagine-*N*-acetylglucosamine linkage, 1 μg of membrane vesicles was digested in 17 μl of solution containing 100 mM phosphate buffer (pH 7.5), 25 mM EDTA, 1% β-mercaptoethanol, 0.5% Nonidet P-40, 1×protease inhibitors and ±0.15 mU *N*-glycosidase F at 37 °C for overnight. The samples, after electrophoresis, were electroblotted to a nitrocellulose membrane and probed with anti-human MRP1 antibodies 42.4 and 897.2.

2.7. Photoaffinity labeling of MRP1 protein

Photoaffinity labeling experiments were performed as described previously [28,29]. The amount of membrane vesicles, ^{32}P-labeled nucleotide, incubation time and temperature are specifically indicated in the figure legends. The labeled proteins were separated on a polyacrylamide gel and electroblotted to a nitrocellulose membrane.

2.8. Membrane vesicle transport

ATP-dependent transport of ^{3}H-labeled leukotriene C4 (LTC4) into the membrane vesicles was assayed by a rapid filtration technique [46,47]. The assays were carried out in a 30 μl solution containing 3 μg of membrane vesicles, 50 mM Tris–HCl (pH 7.5), 250 mM sucrose, 10 mM $MgCl_2$, varying concentrations of LTC4 and varying concentrations of ATP as indicated in the figure legends. AMP was used as a negative control. After incubation at 37 °C for the time indicated in the figure legends, the samples were brought

back to ice and diluted with 1 ml of ice-cold 1× transport buffer (50 mM Tris–HCl, pH 7.5, 250 mM sucrose and 10 mM $MgCl_2$) and filtered on nitrocellulose membranes (0.2 μm) that had been equilibrated with 1× transport buffer. The filter was then washed with 10 ml of ice-cold 1×transport buffer, air-dried and placed in 10 ml of biodegradable counting scintillant (Amersham Pharmacia Biotech). The radioactivity bound to the nitrocellulose membrane was determined by liquid scintillation counting (Beckman LS 6000SC).

3. Results

3.1. Wild-type, NBD1 and NBD2 mutants express similar amounts of MRP1 proteins

Structural analyses of ABC-transporters MJ0796 [40] and HisP [39] indicate that the acidic amino acid directly adjacent to the C-terminal of the aspartic acid residue in Walker B motif may function as a catalytic base during ATP hydrolysis. Fig. 1A shows an alignment of Walker B motifs from several ABC transporters, including MJ0796, HisP, P-gp and MRP1. In order to study the function of each NBD in MRP1 protein, this putative catalytic residue D793 in NBD1 was mutated to E, L or N and E1455 in NBD2 to Q (Fig. 1B). The recombinant viruses expressing wild-type and mutated N-half (1–932) and C-half (933–1531) were prepared and used to infect Sf21 cells. Fig. 1C shows the Western blot results of the proteins expressed in Sf21 cells, probed with antibody 42.4 against NBD1 and 897.2 against NBD2. The antibodies (42.4 and 897.2) detected three bands, 52, 57 and 93 kDa, in the membrane vesicles containing wild-type and mutated N-half+C-half (Fig. 1C). The antibodies detected only a 93 kDa band when the cells were infected with recombinant virus expressing N-half alone (data not shown). Unexpectedly, the antibodies detected two bands, 57 kDa and 52 kDa, when the cells were infected with recombinant virus expressing C-half alone (data not shown). Since neither of these three bands was detected in the membrane vesicles prepared from cells infected with virus without MRP1 cDNA (pDual in Fig. 1C), the 93 kDa band in Fig. 1C must be the N-half fragment and the 57 kDa and 52 kDa, the C-half fragments, which are different from the previously published results [43]. Since our C-half construct is slightly different from the previously published one, we speculated that the two bands were the C-half fragments with two different glycosylation patterns. In order to prove our hypothesis, membrane vesicles containing wild-type N-half and wild-type C-half were digested with *N*-glycosidase F and resolved in SDS-PAGE (Fig. 1D). The lower mobility band was shifted to the higher mobility band after *N*-glycosidase F treatment of the C-half (Fig. 1D, lane 2), confirming that the higher molecular weight protein is glycosylated, whereas the lower molecular weight band is not. The mobility of the N-half is also increased after *N*-glycosidase F treatment (Fig. 1D, lane 2), indicating that the N-half of MRP1 is also glycosylated in Sf21 cells. Fig. 1C shows that the intensity of the N-half band is slightly higher than the C-half. Whether these results imply that the N-half proteins have higher copy numbers than C-half is unclear since different antibodies were used to detect N-half (42.4) and C-half (897.2). However, if we compare the intensity (measured by a densitometer) of wild-type N-half band (co-expressed with wild-type C-half) versus mutated N-halves (co-expressed with wild-type C-half) or wild-type C-half (co-expressed with wild-type N-half) versus mutated C-half (co-expressed with wild-type N-half), the ratios of N-halves are similar to the ratios of the counterpart C-halves. Fig. 1 legend indicates that the mean ratios of the averages of N-halves and C-halves are approximately 1, indicating similar amounts of wild-type and mutated MRP1 proteins in the membrane vesicles. Thus it is reasonable to compare their ATP-dependent solute transport activities.

3.2. ATP binding at NBD1 enhances the non-hydrolyzable ATP analogue AMP–PNP binding to the NBD2s in the glycosylated and un-glycosylated C-halves

Since the ATP-dependent uptake of solute relies upon the association of N-half and C-half proteins [9], whether the N-half of MRP1 protein was associated with the core-glycosylated or un-glycosylated C-half or both was not clear. To test whether NBD1 in N-half will interact with the NBD2 in the core-glycosylated or un-glycosylated or both, membrane vesicles containing wild-type N- and C-halves were labeled with [α-^{32}P]-8-N_3AMP–PNP in the absence or presence of ATP. The rationale of this experiment is based on our finding that ATP binding to the first NBD induces conformational changes of the molecule and enhances nucleotide binding to the second NBD in full-length MRP1 molecule [33]. Fig. 2 shows that the labeling intensity of the N-half containing NBD1 is gradually decreased in the presence of increasing concentrations of ATP. In contrast, the labeling intensities of the core-glycosylated and un-glycosylated C-halves containing NBD2 are gradually increased in the presence of increasing concentrations of ATP, reaching almost five fold in the presence of 80 μM ATP. These results were interpreted as that the two NBDs still interacted each other even though they were not covalently linked and no matter whether the C-half was glycosylated or not, both of them were associated with the co-expressed N-half, making possible that both forms of C-halves contribute to solute transport.

3.3. Substitution of the Asp residue with a non-acidic amino acid in NBD1 increased the K_m and V_{max} values for LTC4 in MRP1 mediated transport

In order to test whether these Walker B mutations, D793E, D793L and D793N in NBD1 and E1455Q in

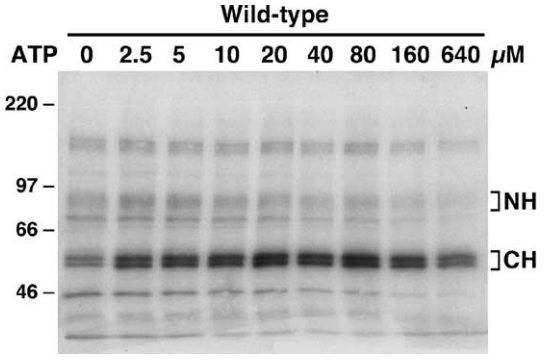

Fig. 2. Labeling intensities of glycosylated and un-glycosylated C-halves were increased in the presence of ATP. Photolabeling experiments were carried out in a 10 μl of solution containing 10 μg membrane vesicles (wild-type N-half and wild-type C-half) and 50 μM [α-^{32}P]-8-N_3AMP–PNP in the absence or presence of ATP indicated on top of the gel. The samples were mixed on ice, transferred to 37 °C water bath for 10 min, brought back to ice and then UV-irradiated (254 nm) for 2 min. The samples were subjected to SDS-PAGE (7%) and electroblotted to a nitrocellulose membrane. Molecular weight markers are indicated on the left. NH and CH on the right indicate the photo-labeled N-half and C-half of MRP1 proteins.

NBD2, affect the kinetics of ATP-dependent LTC4 transport, membrane vesicles prepared from Sf21 cells expressing these variant MRP1s (Fig. 1C) were utilized to determine their ATP-dependent LTC4 transport activities. Fig. 3 shows that E1455Q is almost completely inactivated, consistent with the previously reported result [43]. Interestingly, this result is also similar to that of the double mutant D1454L/E1455L [28] including the mutations of the D1454 residue in the Walker B motif and the putative catalytic base

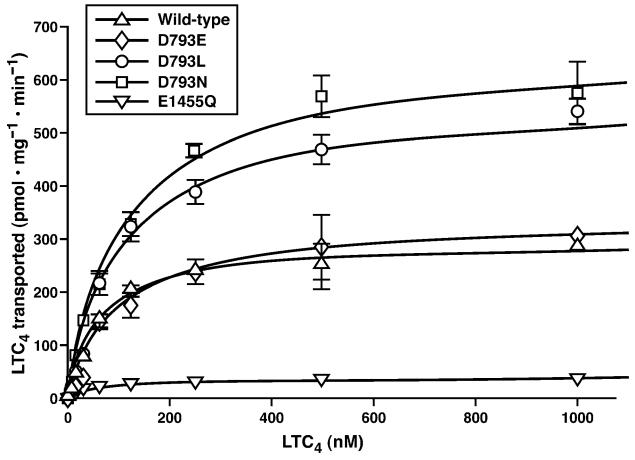

Fig. 3. NBD1 mutants have higher V_{max} and K_m for LTC4 than that of wild-type MRP1. The assays were carried out in a 30 μl solution containing 3 μg of membrane vesicles, 4 mM AMP (as a control) or 4 mM ATP and varying concentrations of LTC4 at 37 °C for 1 min. The amount of LTC4 bound to the membrane vesicles in the presence of 4 mM AMP was subtracted from the corresponding points in the presence of 4 mM ATP. The data are the means±S.D. of triplicate determinations. The samples are: wild-type, wild-type N-half+wild-type C-half; D793E, D793E mutated N-half+wild-type C-half; D793L, D793L mutated N-half+wild-type C-half; D793N, D793N mutated N-half+wild-type C-half and E1455Q, wild-type N-half+E1455Q mutated C-half.

E1455 residue directly adjacent to the D1454, implying that the mutation of the putative catalytic base E1455 to a non-acidic amino acid affecting ATP hydrolysis [43] has the same effects as the D1454L/E1455L double mutant affecting ATP binding [28] and hydrolysis. The mutation of the corresponding residue D793 in NBD1 to the longer arm acidic glutamic acid (D793E) changed the kinetics of ATP-dependent LTC4 transport (Fig. 3). The transport activity of D793E is lower than that of wild-type at lower LTC4 concentrations, consistent with the previously reported results [43]. However, it is slightly higher than that of wild-type at higher LTC4 concentrations, leading to higher V_{max} and K_m (LTC4) values than that of wild-type MRP1 (Table 1). These might be the consequence of the altered properties of this D793E mutated NBD1 [43]. Interestingly, the substitution of the putative catalytic base D793 in NBD1 with a non-acidic amino acid, such as D793L or D793N, increases ATP-dependent LTC4 transport activity (Fig. 3 and Table 1), implying that ATP hydrolysis at NBD1 might not be essential for the transport. In addition, why the substitution with a non-acidic amino acid at this putative catalytic residue leads to higher V_{max} and K_m (LTC4) values (Table 1) is not clear. If we consider the transport reaction as an enzyme catalyzed reaction, LTC4 outside of the vesicles (L_o) is transported into the vesicles (L_i) by MRP1 protein (E),

$$E + L_o \underset{k_{-1}}{\overset{k_1}{\rightleftharpoons}} EL_o \xrightarrow{k_2} E + L_i$$

where $v=k_2[EL_o]$, the rate of EL_o formation$=k_1[E][L_o]$, the rate of EL_o breakdown, including the dissociation from outside of the vesicles and the transportation into the vesicles, $=(k_{-1}+k_2)[EL_o]$, and the Michaelis constant $K_m=(k_{-1}+k_2)/k_1$, which should be affected by different mutations, but not by different amount of enzyme, such as MRP1 protein. In order to have a higher K_m value, either k_2, k_{-1} or both should be increased, or the k_1 value should be decreased. In addition, $V_{max}=k_2[E_T]$, where $[E_T]$ equals the total enzyme concentration, here the total MRP1 protein concentration. Since the amounts of MRP1 proteins in membrane vesicles containing wild-type, D793E, D793L, D793N and E1455Q are similar (Fig. 1C), the much lower V_{max} value of E1455Q than that of the wild-type (Table 1), although the amount of E1455Q (ratio of 0.921) is slightly less than wild-type, indicates a greatly decreased k_2 value, which is perhaps directly associated with the greatly diminished ATPase activity at

Table 1
K_m and V_{max} values (LTC_4) of wild-type and mutant MRP1s

Sample		K_m (nM LTC_4)[a]	V_{max} (pmol LTC_4 mg^{-1} min^{-1})
N-half	C-half		
Wild-type	Wild-type	59±1	287.5±7.5
D793E	Wild-type	110±10	365.0±25.0
D793L	Wild-type	100±0	560.0±0.0
D793N	Wild-type	105±5	575.0±75.0
Wild-type	E1455Q	50±0	37.5±0.5

[a] The K_m values (n=2) and V_{max} values (n=2) were derived from Fig. 3.

the E1455Q mutated NBD2 as shown in Fig. 7M and O; whereas the higher V_{max} value (Table 1) of D793L (a ratio of 0.993 indicates that the amount of D793L is slightly less than wild-type) or D793N (ratio of 1.151) indicates a slightly increased k_2 value, leading to a higher K_m (LTC4) value and a higher rate of ATP-dependent LTC4 transport.

3.4. Combination of D793E, D793L or D793N mutated NBD1 with E1455Q mutated NBD2 does not enhance ATP-dependent LTC4 transport activity

The k_2 values should be directly associated with the rates of ATP hydrolysis by variant MRP1 mutants. The greatly decreased k_2 value for E1455Q is interpreted as that mutation of the putative catalytic E1455 residue to a non-acidic amino acid greatly diminishes the rate of ATP hydrolysis at the mutated NBD2. Whereas the moderately increased k_2 values for D793L and D793N could be interpreted in the following two ways: (1) The mutation of the putative catalytic base D793 to a non-acidic amino acid, such as L or N, somehow increases the rate of ATP hydrolysis at the mutated NBD1 and enhances ATP-dependent LTC4 transport; (2) The mutation of the putative catalytic base D793 to a non-acidic amino acid, such as L or N, decreases the affinity for ATP and increases the release rate of the bound nucleotide from the mutated NBD1. The release of the bound ATP from NBD1 may bring the MRP1 protein back to the original conformation so that the molecule can start a new cycle of ATP-dependent solute transport. In order to test these two possibilities, the D793E, D793L or D793N mutated N-half was co-expressed with the E1455Q mutated C-half. Fig. 4A shows the amounts of proteins expressed in the membrane vesicles prepared from infected Sf21 cells. The results in Fig. 4B show that all the mutants, including wild-type N-half+E1455Q mutated C-half, D793E mutated N-half+E1455Q mutated C-half, D793L mutated N-half+E1455Q mutated C-half and D793N mutated N-half+E1455Q mutated C-half, have similar ATP-dependent LTC4 transport activities. These observations exclude the above given first possible interpretation and support the second possible interpretation.

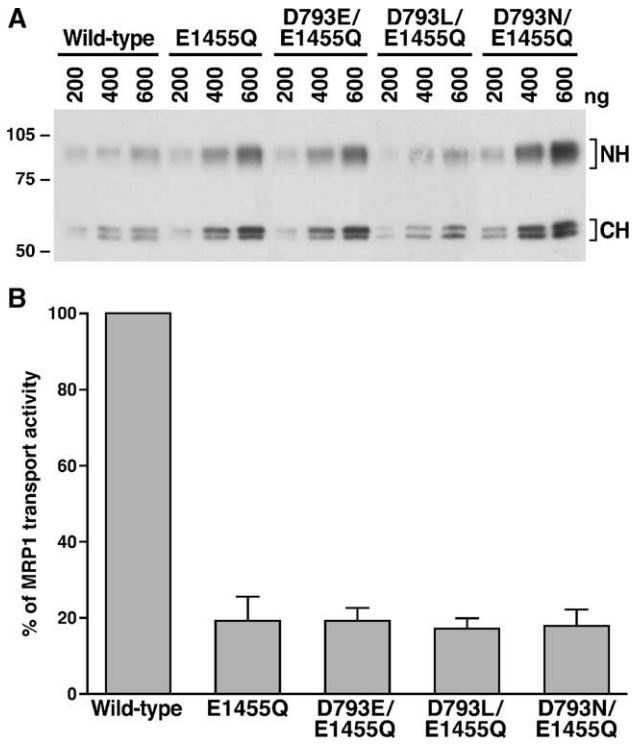

Fig. 4. D793E, D793L or D793N mutated NBD1 does not enhance the ATP-dependent LTC4 transport activity of E1455Q mutated NBD2. (A) Expression of wild-type and double mutant MRP1 proteins in Sf21 cells. Western blot experiments were performed as described in Fig. 1C. The mean ratios of the protein expressions including N-half and C-half are: 1.33±0.11 (E1455Q), 1.49±0.13 (D793E/E1455Q), 0.98±0.05 (D793L/E1455Q) and 1.88±0.29 (D793N/E1455Q). (B) ATP-dependent membrane vesicle transport by wild-type and double mutants. The experiments were performed according to the procedure described in Materials and methods by using the same amount of MRP1 protein in a total of 3 μg of membrane vesicle proteins (adjusted by adding varying amounts of membrane vesicles prepared from Sf21 cells infected with pDual).

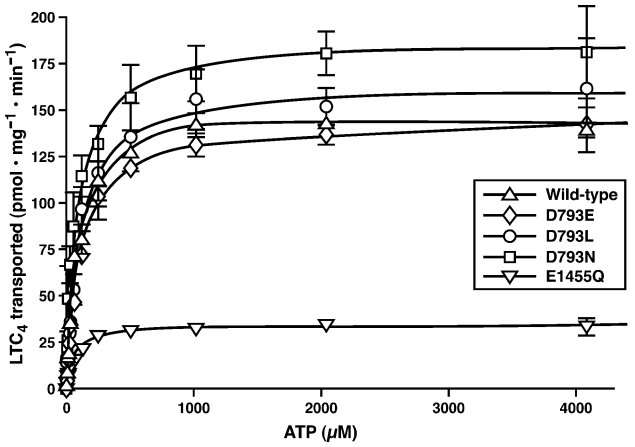

Fig. 5. NBD1 mutants have higher K_m for ATP than that of wild-type MRP1. The assays were carried out in a 30 μl solution containing 3 μg of membrane vesicles, 200 nM LTC4 and varying concentrations of ATP at 37 °C for 1 min. The data are the means±S.D. of triplicate determinations. The samples are: wild-type, wild-type N-half+wild-type C-half; D793E, D793E mutated N-half+wild-type C-half; D793L, D793L mutated N-half+wild-type C-half; D793N, D793N mutated N-half+wild-type C-half and E1455Q, wild-type N-half+E1455Q mutated C-half.

Table 2
K_m values (ATP) of wild-type and mutant MRP1s

Sample		K_m (μM ATP)[a]
N-half	C-half	
Wild-type	Wild-type	72.2±1.6
D793E	Wild-type	106.0±9.7
D793L	Wild-type	107.0±7.5
D793N	Wild-type	92.0±12.5
Wild-type	E1455Q	55.0±0.0

[a] K_m values (for wild-type, D793E, D793L and D793N, n=5; for E1455Q, n=2) were derived from corresponding Michaelis–Menten curves shown in Fig. 5.

3.5. Substitution of D793 with a non-acidic amino acid increases the release rate of bound nucleotide from the mutated NBD1

As mentioned above that the results in Fig. 4B support the second possibility that the mutation of the acidic D793 residue to a non-acidic amino acid, such as L or N, decreases the affinity for ATP and increases the release rate of the bound ATP from the mutated NBD1. To further test this possibility, ATP-dependent LTC4 transport assays were performed in 30 μl solution containing 200 nM LTC4 and varying concentrations of ATP (Fig. 5). The Michaelis constant K_m values for ATP (Table 2) were determined from Fig. 5. The K_m (ATP) value of E1455Q, the putative catalytic base mutant in NBD2, is slightly less than that of wild-type (Table 2), whereas the K_m (ATP) values of D793E, D793L and D793N are slightly higher than that of wild-type (Table 2). Since there are two NBDs in MRP1, K_m (ATP) values should reflect the sum of the K_m (ATP) values from NBD1 and NBD2. In addition, the two NBDs may interact with each other during ATP-dependent solute transport [28,33,48–50] and affect their individual K_ms, making the two K_ms difficult to be separated. However, we can simplify the working process and consider each NBD separately. Each NBD may catalyze the following reactions:

$$\mathrm{ATP} + \mathrm{NBD} \underset{k_{-1}}{\overset{k_1}{\rightleftharpoons}} \mathrm{ATP}\cdot\mathrm{NBD} \xrightarrow{k_2} \mathrm{NBD} + \mathrm{ADP} + \mathrm{P_i}$$

where the individual Michaelis constant $K_m=(k_{-1}+k_2)/k_1$. A higher K_m (ATP) value means that either the k_{-1}, k_2 or both are increased, or the k_1 value is decreased. Although the two K_m (ATP) values of NBD1 and NBD2 derived from ATP-dependent LTC4 transport cannot be separated, the K_d (ATP) values determined from ATP binding on ice can be easily separated. Since the reactions were performed on ice, ATP hydrolysis should be greatly diminished and the allosteric effect of ATP binding to NBD1 on the nucleotide binding to NBD2 should also be greatly diminished [51]. Therefore the binding should mainly reflect the equilibrium of forwarding and reversing reactions:

$$\mathrm{ATP} + \mathrm{NBD} \underset{k_{-1}}{\overset{k_1}{\rightleftharpoons}} \mathrm{ATP}\cdot\mathrm{NBD}$$

where $K_d=k_{-1}/k_1$. In order to interpret the results in Table 2, membrane vesicles containing wild-type and mutant MRP1s were used to bind ATP on ice with varying concentrations of [α-^{32}P]-8-N_3ATP. Fig. 6A, D, G, J and M show the autoradiograms reflecting [α-^{32}P]-8-N_3ATP labeling of wild-type, D793E, D793L, D793N and E1455Q. Labeling was quantified by Packard Instant Imager and plotted against the concentration of [α-^{32}P]-8-N_3ATP (Fig. 6B, C, E, F, H, I, K, L, N and O). K_ds (ATP) were determined from Fig. 6 and listed in Table 3. The K_d (ATP) value for D793E mutated NBD1, co-expressed with wild-type NBD2, is slightly less than that of wild-type NBD1 (Table 3), implying moderately increased affinity for ATP. However, the K_d (ATP) value for wild-type NBD2 co-expressed with D793E mutated NBD1 is slightly higher than that of the wild-type NBD2 co-expressed with wild-type NBD1, implying that the D793E mutated NBD1 has an effect on the wild-type NBD2. The K_d (ATP) values for D793L and D793N mutated NBD1 co-expressed with wild-type NBD2 are almost three fold higher than that of wild-type NBD1 (Table 3), implying that the mutation of this acidic D793 residue to a non-acidic amino acid decreased k_1 (lower rate of binding) and/or increased k_{-1} (higher rate of releasing), i.e. lower affinity. The mutation of D793L or D793N does not have a significant effect on the wild-type NBD2 (Table 3). The K_d for E1455Q mutated NBD2 co-expressed with wild-type NBD1 is almost five fold higher than that of wild-type NBD2 (Table 3), implying that the substitution of the putative catalytic E1455 residue with a non-acidic amino acid decreased k_1 (lower rate of binding) and/or increased k_{-1} (higher rate of releasing), i.e. lower affinity. In contrast to the counterpart NBD1 mutants D793N and D793L, the substitution of the E1455 with a non-acidic amino acid has an effect on the wild-type NBD1 (Table 3).

3.6. The substitution of the putative catalytic D793 residue with a non-acidic amino acid increases release rate of the bound ATP

The higher K_d (ATP) values of D793L and D793N mutated NBD1 were interpreted as that the binding rate was decreased whereas the release rate of the bound ATP was increased. We thought about ways to directly measure the release rate of the bound ATP. For example, after removing the un-bound nucleotide by washing with cold buffer, the samples were re-suspended in buffer, incubated for varying times and then UV-photolabeled the remaining ATP. However, due to trace amount of labeling in the absence of vanadate after washing [28], the experiments were impracticable. We then decided to do the experiments without washing, as described in Fig. 7. Since the initial labeling was performed on ice without washing out the un-bound nucleotide and then shifted to 37 °C for varying times, the bound nucleotide may be either released without hydrolysis or hydrolyzed and then released. Of course, the empty-handed NBDs may bind the nucleotide and release again until the [γ-^{32}P]-8-N_3ATP in the solution is exhausted due to the ATPases in the membrane vesicles. Therefore, the time required to lose 50% of the labeling may reflect the k_1, k_{-1} and k_2 levels of a specific NBD. Fig. 7A, D, G, J and M show the autoradiograms reflecting [γ-^{32}P]-8-N_3ATP labeling of wild-type, D793E, D793L, D793N and E1455Q. Labeling was quantified by Packard Instant Imager and plotted against the incubation time (Fig. 7B, C, E, F, H, I, K, L, N and O). The time required to lose 50% of the labeling was determined from Fig. 7 and listed in Table 4. As

expected, most of the labeling disappeared within a short time, except for the E1455Q mutated NBD2 (Fig. 7M and O). The labeling with [γ-^{32}P]-8-N_3ATP at the C-half containing E1455Q mutated NBD2 is increased almost three fold within 2 min incubation at 37 °C and the $T_{1/2}$ of this mutated NBD2 is much longer than that of wild-type (Table 4). These results indicate that: (1) ATP binding at the wild-type NBD1 induces conformational changes of the protein [33] and enhances the nucleotide binding (increases k_1 or affinity for ATP, leading to

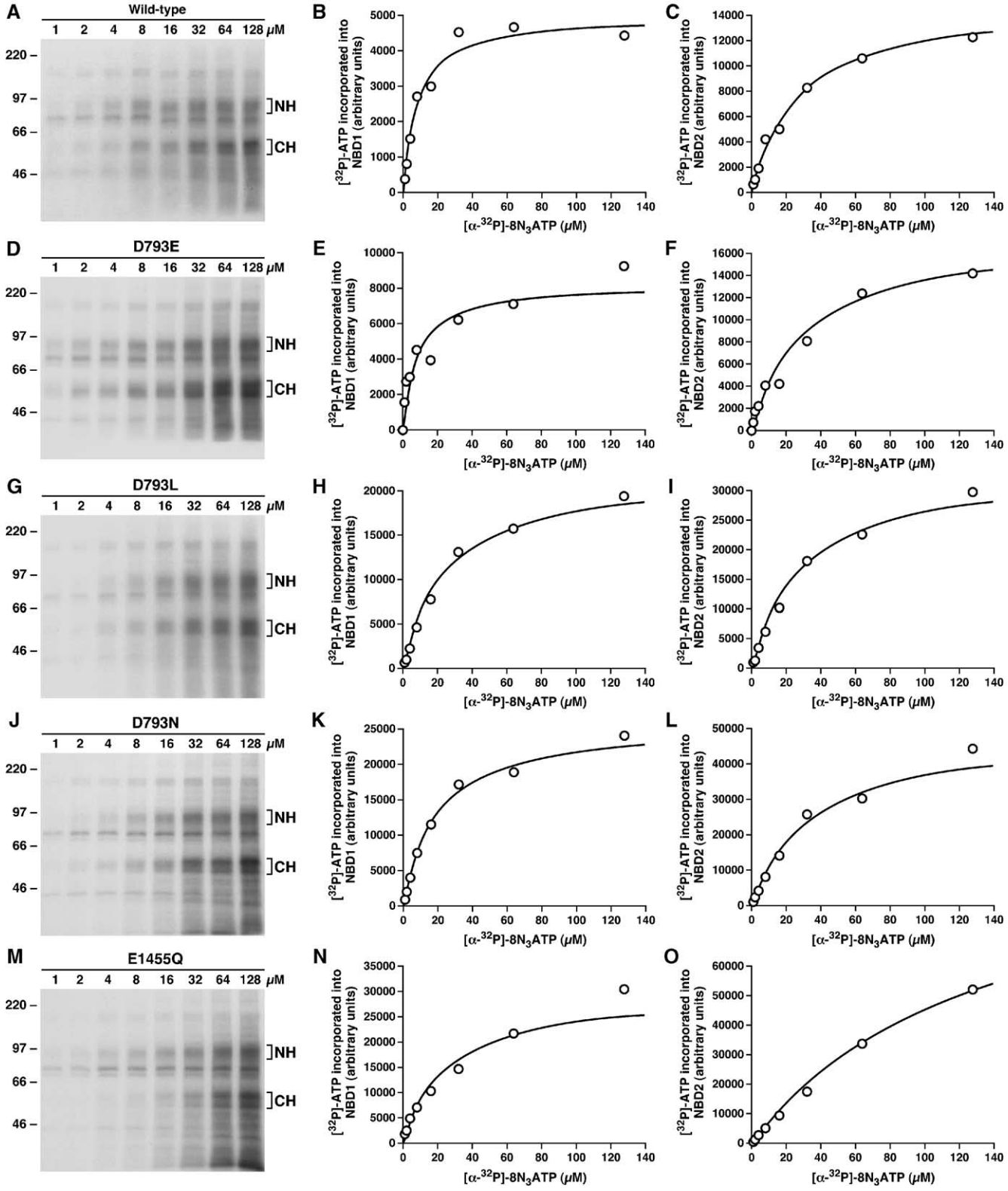

Table 3
Substitution of D793 with a non-acidic amino acid decreases affinity for ATP

Sample		K_d of NBD1 (μM ATP)[a]	K_d of NBD2 (μM ATP)
N-half	C-half		
Wild-type	Wild-type	11.7±2.8	32.7±2.3
D793E	Wild-type	7.8±4.1	41.0±8.1
D793L	Wild-type	30.5±2.5	32.9±1.9
D793N	Wild-type	28.4±4.5	33.7±0.7
Wild-type	E1455Q	19.4±3.3	155.8±9.0

[a] The K_d (μM ATP) values (for wild-type, n=12; D793E, n=9; D793L and E1455Q, n=5; D793N, n=8) were derived from Fig. 6.

decreased K_d) at the E1455Q mutated NBD2 at 37 °C, consistent with our previous finding [51]; (2) the bound ATP at the E1455Q mutated NBD2 cannot be efficiently hydrolyzed due to the substitution of the putative catalytic acidic residue with a non-acidic amino acid (greatly decreased k_2); (3) the release rate of the bound ATP from this mutated NBD2 is much lower (decreased k_{-1}) than that of wild-type, leading to a longer $T_{1/2}$ value (Table 4). The combination of increased k_1 and decreased k_{-1} and k_2 leads to a decreased K_m (ATP) value (Table 2). In addition, the $T_{1/2}$ value for the wild-type NBD1 co-expressed with E1455Q mutated NBD2 is slightly longer than that of wild-type N-half co-expressed with the wild-type C-half (Table 4), perhaps reflecting the stabilization effect of the bound nucleotide at NBD1 by the occluded nucleotide at NBD2 [28]. These results are consistent with the lower K_m (ATP) value of E1455Q than that of the wild-type (Table 2) and the low ability to transport LTC4 (Figs. 3 and 5). In the cases of D793E, D793L and D793N, the $T_{1/2}$ values (for NBD1 and NBD2) are shorter than that of the wild-type and E1455Q (Table 4). No matter whether these are due to a decreased k_1 and/or increased k_{-1} or k_{-1}+k_2, these results are consistent with their increased K_m (ATP) values (Table 2).

4. Discussion

MRP1 protein couples ATP binding/hydrolysis to solute transport by utilizing its NBDs and transmembrane domains. However, the sequences of the two NBDs are quite different [15] and, therefore, they may play different roles during ATP-dependent solute transport. Indeed, NBD1 has slightly higher affinity for ATP than that of NBD2 [34], whereas NBD2 has much higher ATPase activity than that of NBD1 [27,28,30]. In addition, ATP binding at NBD1 causes conformational changes of the MRP1 molecule and enhances nucleotide binding at NBD2 [33], whereas vanadate-dependent ADP trapping at NBD2 stabilizes the bound ATP at NBD1 [28]. We have further shown that ATP binding to NBD1 plays a regulatory role whereas ATP hydrolysis at NBD2 plays a dominant role in ATP-dependent solute transport [34]. All these results demonstrated that ATP hydrolysis at NBD2 is the major determinant of solute transport. Although ATP bound to NBD1 of MRP1 may be hydrolyzed [43], it is unclear whether this hydrolysis is essential for transport.

Structural analysis of ABC transporters, such as HisP [39] or MJ0796 [40], suggested that the acidic amino acid directly adjacent to the C-terminal of the Asp residue in the Walker B motif may activate a water molecule to attack the gamma phosphate of the ATP bound to this NBD, leading to hydrolysis. The mutation of this putative catalytic base in bacterial ABC transporters MJ0796 [41] and HisP [39] or in mouse P-gp [42] abolished ATP-dependent solute transport. The substitution of the counterpart putative catalytic residue E1455 with a non-acidic amino acid (E1455Q) almost completely abolished the ATP-dependent LTC4 transport (Figs. 3 and 5), presumably due to the greatly decreased ATPase activity of this E1455Q mutated NBD2 (Fig. 7M and O). The substitution of this putative catalytic residue E1455 with a shorter spacer-arm negatively charged Asp residue increased affinity for ATP but greatly decreased its ability to hydrolyze ATP, leading to abolish the ATP-dependent LTC4 transport [43]. All these results support the notion that ATP hydrolysis at the NBD2 of human MRP1 is essential for the ATP-dependent solute transport. In contrast, the substitution of the putative catalytic residue D793 in NBD1 of human MRP1 with a non-acidic amino acid did not have a significant effect on the rate of ATP-dependent LTC4 transport (Figs. 3 and 5 and [43]). In addition, the substitution of this putative catalytic residue D793 with a longer spacer-arm negatively charged Glu enhances its hydrolytic capacity [43], but does not increase the ATP-dependent solute transport activity of D793E/E1455Q mutated MRP1 (Fig. 4) or markedly

Fig. 6. D793L and D793N mutated NBD1s have higher K_d values than that of wild-type. The photolabeling experiments were carried out in a 10 μl of solution containing 10 μg MRP1 membrane vesicles and varying concentration of [α-^{32}P]-8-N_3ATP on ice for 10 min. The reaction mixture was UV-irradiated on ice for 2 min, subjected to SDS-PAGE (7%) and electroblotted to a nitrocellulose membrane. Molecular weight markers are indicated on the left. NH and CH on the right indicate the photo-labeled N-half and C-half of MRP1 proteins. A, D, G, J, and M: Autoradiograms of [α-^{32}P]-8-N_3ATP labeled wild-type N-half co-expressed with wild-type C-half; D793E mutated N-half+wild-type C-half; D793L mutated N-half+wild-type C-half; D793N mutated N-half+wild-type C-half; and wild-type N-half+E1455Q mutated C-half. B and C: Plot of the amount of [α-^{32}P]-8-N_3ATP incorporated into wild-type N-half (B) co-expressed with wild-type C-half (C). The amounts of [α-^{32}P]-8-N_3ATP incorporated into the N-half (NBD1) and C-half (NBD2) fragments were measured by Packard Instant Imager and plotted out against [α-^{32}P]-8-N_3ATP concentration. E and F: D793E mutated N-half (E) co-expressed with wild-type C-half (F). H and I: D793L mutated N-half (H) co-expressed with wild-type C-half (I). K and L: D793N mutated N-half (K) co-expressed with wild-type C-half (L). N and O: Wild-type N-half (N) co-expressed with E1455Q mutated C-half (O).

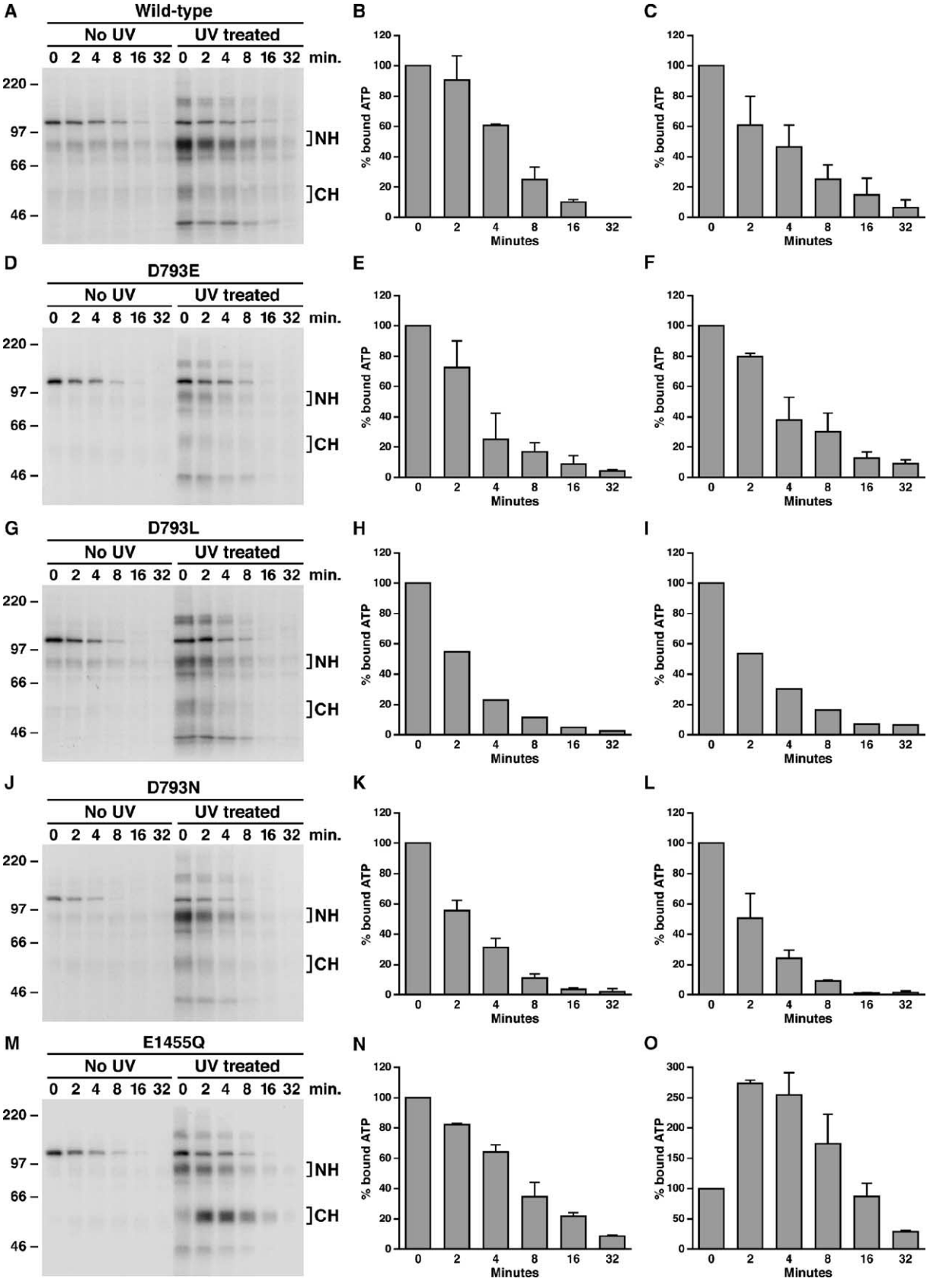
A
Wild-type
No UV
UV treated
0 2 4 8 16 32 0 2 4 8 16 32 min.
220 –
97 –
66 –
46 –
]NH
]CH
B
C
% bound ATP
Minutes
D
D793E
E
F
G
D793L
H
I
J
D793N
K
L
M
E1455Q
N
O

Table 4
Release rate of the bound nucleotide at the wild-type and mutated NBDs

Sample		$T_{1/2}$ of NBD1 (min)[a]	$T_{1/2}$ of NBD2 (min)
N-half	C-half		
Wild-type	Wild-type	5.3±0.3	3.7±2.0
D793E	Wild-type	3.0±0.7	3.4±1.0
D793L	Wild-type	2.3	2.3
D793N	Wild-type	2.5±0.5	2.2±0.7
Wild-type	E1455Q	6.1±0.3	25.6±2.4

[a] The $T_{1/2}$ value (for wild-type, D793E, D793N and E1455Q, n=3; for D793L, n=1) is the time required to release 50% of the bound nucleotide and was derived from Fig. 7.

decreases the ATP-dependent LTC4 (at 50 nM) transport activity [43], implying that ATP hydrolysis at the NBD1 of human MRP1 protein may not be essential for the ATP-dependent solute transport.

The ATP-dependent LTC4 transport activity of the co-expressed N-half and C-half is much less active than the intact MRP1 [9]. We were curious whether this low transport activity of the co-expressed N-half+C-half was due to the weakened interactions between the two halves. Membrane vesicles containing wild-type N-half+C-half were photolabeled with [α-^{32}P]-8-N_3AMP–PNP in the absence or presence of ATP (Fig. 2). The labeling intensities of the core-glycosylated and un-glycosylated C-halves were gradually increased along with the increased concentration of ATP, reaching almost five fold in the presence of 80 μM ATP (Fig. 2), indicating that ATP binding to NBD1 in N-half still induces conformational changes of the NBD2 in C-half. However, the ATP concentration required to have a maximum enhancement effect increased from 10 μM ([33], for the intact MRP1) to 80 μM (Fig. 2, for the co-expressed N-half+C-half), implying that the enhancement effect is weakened in the co-expressed halves.

It is clear that these mutations not only change the structure in that specific site, but also the properties of the protein. The substitution of the putative catalytic E1455 with a non-acidic amino acid Q greatly increased the K_d (ATP) of the E1455Q mutated NBD2 (Fig. 6 and Table 3), meaning increased k_{-1} and decreased k_1 on ice. This E1455Q mutation at NBD2 also has a negative effect on the co-expressed wild-type NBD1, leading to the increased K_d (Table 3), indicating the increased k_{-1} and decreased k_1 on ice. However, the properties of the E1455Q mutated protein at 37 °C are different from that on ice. The [γ-^{32}P]-8-N_3ATP bound to the E1455Q mutated NBD2 cannot be efficiently hydrolyzed (greatly decreased k_2) but occluded there (decreased k_{-1}) (Fig. 7M and Table 4); in the meantime, the occluded [γ-^{32}P]-8-N_3ATP at the E1455Q mutated NBD2 stabilized the bound [γ-^{32}P]-8-N_3ATP [28] at the wild-type NBD1 co-expressed with the E1455Q mutated NBD2 (Fig. 7N), meaning decreased k_{-1}; all these changes lead to a decreased K_m (ATP) value and an inability to transport LTC4 (Table 1 and 2). In contrast, interestingly, the substitution of the putative catalytic residue D793 in NBD1 with a non-acidic amino acid, such as D793L or D793N, increased the rate of ATP-dependent LTC4 transport ([29] and Fig. 3). This radical substitution increased the K_d (ATP) values of the D793L or D793N mutated NBD1 (Fig. 6 and Table 3), where K_d=k_{-1}/k_1, since ATP hydrolysis on ice is limited. The increased K_d of D793N or D793L means increased k_{-1}, in other words, increased releasing rate of the bound ATP, and/or decreased k_1, in other words, decreased the rate of ATP binding. The time required to lose 50% of the bound ATP from the D793L or D793N mutated NBD1 and the co-expressed wild-type NBD2 is much shorter than that of the wild-type (Fig. 7 and Table 4), implying the increased k_{-1} and/or decreased k_1 values. All these results (on ice or at 37 °C) are consistent with the increased K_m (ATP) values in ATP-dependent LTC4 transport (Table 2). These results were interpreted as that the substitution of the acidic amino acid D793 with a non-charged residue decreased the affinity for ATP, meaning that decreased rate of ATP binding and increased the release rate of the bound nucleotide from the mutated NBD1, and the releasing of the bound nucleotide from NBD1 brought the protein back to its original conformation so that the molecule could start a new cycle of ATP-dependent solute transport. This hypothesis is supported by our recent results that the substitution of the aromatic W653 residue in NBD1 of MRP1 interacting with the adenine ring of the bound ATP with a polar cysteine residue greatly decreases affinity for ATP (increased K_d value) and increases K_m (ATP) values, leading to much higher V_{max} (LTC4) values [52].

Fig. 7. E1455Q mutated NBD2 greatly diminishes the rate of ATP hydrolysis at the mutated NBD2. The photolabeling experiments were carried out in a 10 μl of solution containing 10 μg MRP1 membrane vesicles and 10 μM [γ-^{32}P]-8-N_3ATP. The samples were mixed on ice, incubated on ice for 10 min and then transferred to 37 °C water bath for 0, 2, 4, 8, 16 and 32 min. The samples were brought back to ice after the indicated incubation time at 37 °C. One of the two samples was immediately UV-irradiated for 2 min whereas another was not, as shown on top of the gel. The samples were subjected to SDS-PAGE and electroblotted to a nitrocellulose membrane. Molecular weight markers are indicated on the left. NH and CH on the right indicate the photo-labeled N-half and C-half of MRP1 proteins. A, D, G, J, and M: Autoradiograms of [γ-^{32}P]-8-N_3ATP labeled wild-type N-half co-expressed with wild-type C-half; D793E mutated N-half+wild-type C-half; D793L mutated N-half+wild-type C-half; D793N mutated N-half+wild-type C-half; and wild-type N-half+E1455Q mutated C-half. B and C: Plot of the amount of [γ-^{32}P]-8-N_3ATP incorporated into wild-type N-half (B) co-expressed with wild-type C-half (C). The amounts of [γ-^{32}P]-8-N_3ATP incorporated into N-half (NBD1) or C-half (NBD2) were measured by Packard Instant Imager. The amounts of the radioactivity in the samples without UV-treatment were considered as background and subtracted from corresponding samples treated with UV-irradiation. The amounts of radioactivity in the sample without undergoing 37 °C incubation were considered as 100%. E and F: D793E mutated N-half (E) co-expressed with wild-type C-half (F). H and I: D793L mutated N-half (H) co-expressed with wild-type C-half (I). K and L: D793N mutated N-half (K) co-expressed with wild-type C-half (L). N and O: Wild-type N-half (N) co-expressed with E1455Q mutated C-half (O).

Acknowledgements

We thank Sharon Fleck for the preparation of the manuscript and Marv Ruona for preparation of the graphics.

References

[1] F.J. Sharom, R. Liu, Y. Romsicki, Spectroscopic and biophysical approaches for studying the structure and function of the P-glycoprotein multidrug transporter, Biochem. Cell. Biol. 76 (1998) 695–708.
[2] A.H. Schinkel, P. Borst, Multidrug resistance mediated by P-glycoproteins, Semin. Cancer Biol. 2 (1991) 213–226.
[3] M. Horio, M.M. Gottesman, I. Pastan, ATP-dependent transport of vinblastine in vesicles from human multidrug-resistant cells, Proc. Natl. Acad. Sci. U. S. A. 85 (1988) 3580–3584.
[4] M. Muller, C. Meijer, G.J. Zaman, P. Borst, R.J. Scheper, N.H. Mulder, E.G. de Vries, P.L. Jansen, Overexpression of the gene encoding the multidrug resistance-associated protein results in increased ATP-dependent glutathione S-conjugate transport, Proc. Natl. Acad. Sci. U. S. A. 91 (1994) 13033–13037.
[5] I. Leier, G. Jedlitschky, U. Buchholz, S.P. Cole, R.G. Deeley, D. Keppler, The MRP gene encodes an ATP-dependent export pump for leukotriene C4 and structurally related conjugates, J. Biol. Chem. 269 (1994) 27807–27810.
[6] M. Muller, E.G. de Vries, P.L. Jansen, Role of multidrug resistance protein (MRP) in glutathione S-conjugate transport in mammalian cells, J. Hepatol. 24 (1996) 100–108.
[7] D.W. Loe, R.G. Deeley, S.P. Cole, Characterization of vincristine transport by the M(r) 190,000 multidrug resistance protein (MRP): evidence for cotransport with reduced glutathione, Cancer Res. 58 (1998) 5130–5136.
[8] B.D. Stride, C.E. Grant, D.W. Loe, D.R. Hipfner, S.P.C. Cole, R.G. Deeley, Pharmacological characterization of the murine and human orthologs of multidrug-resistance protein in transfected human embryonic kidney cells, Mol. Pharmacol. 52 (1997) 344–353.
[9] M. Gao, D.W. Loe, C.E. Grant, S.P.C. Cole, R.G. Deeley, Reconstitution of ATP-dependent leukotriene C4 transport by co-expression of both half-molecules of human multidrug resistance protein in insect cells, J. Biol. Chem. 271 (1996) 27782–27787.
[10] D. Keppler, I. Leier, G. Jedlitschky, R. Mayer, M. Buchler, The function of the multidrug resistance proteins (MRP and cMRP) in drug conjugate transport and hepatobiliary excretion, Adv. Enzyme Regul. 36 (1996) 17–29.
[11] D. Lautier, Y. Canitrot, R.G. Deeley, S.P. Cole, Multidrug resistance mediated by the multidrug resistance protein (MRP) gene, Biochem. Pharmacol. 52 (1996) 967–977.
[12] D.W. Loe, K.C. Almquist, S.P. Cole, R.G. Deeley, ATP-dependent 17 beta-estradiol 17-(beta-D-glucuronide) transport by multidrug resistance protein (MRP). Inhibition by cholestatic steroids, J. Biol. Chem. 271 (1996) 9683–9689.
[13] C.J. Chen, J.E. Chin, K. Ueda, D.P. Clark, I. Pastan, M.M. Gottesman, I.B. Roninson, Internal duplication and homology with bacterial transport proteins in the mdr1 (P-glycoprotein) gene from multidrug-resistant human cells, Cell 47 (1986) 381–389.
[14] E. Georges, T. Tsuruo, V. Ling, Topology of P-glycoprotein as determined by epitope mapping of MRK-16 monoclonal antibody, J. Biol. Chem. 268 (1993) 1792–1798.
[15] S.P. Cole, G. Bhardwaj, J.H. Gerlach, J.E. Mackie, C.E. Grant, K.C. Almquist, A.J. Stewart, E.U. Kurz, A.M. Duncan, R.G. Deeley, Overexpression of a transporter gene in a multidrug-resistant human lung cancer cell line [see comments], Science 258 (1992) 1650–1654.
[16] S.V. Ambudkar, C.O. Cardarelli, I. Pashinsky, W.D. Stein, Relation between the turnover number for vinblastine transport and for vinblastine-stimulated ATP hydrolysis by human P-glycoprotein, J. Biol. Chem. 272 (1997) 21160–21166.
[17] A.E. Senior, Catalytic mechanism of P-glycoprotein, Acta Physiol. Scand., Suppl. 643 (1998) 213–218.
[18] A.E. Senior, M.K. al-Shawi, I.L. Urbatsch, ATPase activity of Chinese hamster P-glycoprotein, Methods Enzymol. 292 (1998) 514–523.
[19] I.L. Urbatsch, B. Sankaran, J. Weber, A.E. Senior, P-glycoprotein is stably inhibited by vanadate-induced trapping of nucleotide at a single catalytic site, J. Biol. Chem. 270 (1995) 19383–19390.
[20] I.L. Urbatsch, B. Sankaran, S. Bhagat, A.E. Senior, Both P-glycoprotein nucleotide-binding sites are catalytically active, J. Biol. Chem. 270 (1995) 26956–26961.
[21] M. Azzaria, E. Schurr, P. Gros, Discrete mutations introduced in the predicted nucleotide-binding sites of the mdr1 gene abolish its ability to confer multidrug resistance, Mol. Cell. Biol. 9 (1989) 5289–5297.
[22] I.L. Urbatsch, L. Beaudet, I. Carrier, P. Gros, Mutations in either nucleotide-binding site of P-glycoprotein (Mdr3) prevent vanadate trapping of nucleotide at both sites, Biochemistry 37 (1998) 4592–4602.
[23] A.E. Senior, S. Bhagat, P-glycoprotein shows strong catalytic cooperativity between the two nucleotide sites, Biochemistry 37 (1998) 831–836.
[24] C.A. Hrycyna, M. Ramachandra, U.A. Germann, P.W. Cheng, I. Pastan, M.M. Gottesman, Both ATP sites of human P-glycoprotein are essential but not symmetric, Biochemistry 38 (1999) 13887–13899.
[25] C. Vigano, M. Julien, I. Carrier, P. Gros, J.M. Ruysschaert, Structural and functional asymmetry of the nucleotide-binding domains of P-glycoprotein investigated by attenuated total reflection Fourier transform infrared spectroscopy, J. Biol. Chem. 277 (2002) 5008–5016.
[26] L. Beaudet, P. Gros, Functional dissection of P-glycoprotein nucleotide-binding domains in chimeric and mutant proteins. Modulation of drug resistance profiles, J. Biol. Chem. 270 (1995) 17159–17170.
[27] M. Gao, H.R. Cui, D.W. Loe, C.E. Grant, K.C. Almquist, S.P. Cole, R.G. Deeley, Comparison of the functional characteristics of the nucleotide binding domains of multidrug resistance protein 1, J. Biol. Chem. 275 (2000) 13098–13108.
[28] Y. Hou, L. Cui, J.R. Riordan, X.B. Chang, Allosteric interactions between the two non-equivalent nucleotide binding domains of multidrug resistance protein MRP1, J. Biol. Chem. 275 (2000) 20280–20287.
[29] L. Cui, Y.X. Hou, J.R. Riordan, X.B. Chang, Mutations of the Walker B motif in the first nucleotide binding domain of multidrug resistance protein MRP1 prevent conformational maturation, Arch. Biochem. Biophys. 392 (2001) 153–161.
[30] K. Nagata, M. Nishitani, M. Matsuo, N. Kioka, T. Amachi, K. Ueda, Nonequivalent nucleotide trapping in the two nucleotide binding folds of the human multidrug resistance protein MRP1, J. Biol. Chem. 275 (2000) 17626–17630.
[31] Z.E. Sauna, S.V. Ambudkar, Characterization of the catalytic cycle of ATP hydrolysis by human P-glycoprotein. The two ATP hydrolysis events in a single catalytic cycle are kinetically similar but affect different functional outcomes, J. Biol. Chem. 276 (2001) 11653–11661.
[32] Z.E. Sauna, S.V. Ambudkar, Evidence for a requirement for ATP hydrolysis at two distinct steps during a single turnover of the catalytic cycle of human P-glycoprotein, Proc. Natl. Acad. Sci. U. S. A. 97 (2000) 2515–2520.
[33] Y.X. Hou, L. Cui, J.R. Riordan, X.B. Chang, ATP binding to the first nucleotide-binding domain of multidrug resistance protein MRP1 increases binding and hydrolysis of ATP and trapping of ADP at the second domain, J. Biol. Chem. 277 (2002) 5110–5119.
[34] R. Yang, L. Cui, Y.-X. Hou, J.R. Riordan, X.B. Chang, ATP binding to the first nucleotide binding domain of multidrug resistance-associated protein plays a regulatory role at low nucleotide concentration, whereas ATP hydrolysis at the second plays a dominant role in ATP-dependent leukotriene C4 transport, J. Biol. Chem. 278 (2003) 30764–30771.

[35] M. Matsuo, N. Kioka, T. Amachi, K. Ueda, ATP binding properties of the nucleotide-binding folds of SUR1, J. Biol. Chem. 274 (1999) 37479–37482.
[36] K. Szabo, G. Szakacs, T. Hegeds, B. Sarkadi, Nucleotide occlusion in the human cystic fibrosis transmembrane conductance regulator. Different patterns in the two nucleotide binding domains, J. Biol. Chem. 274 (1999) 12209–12212.
[37] L. Aleksandrov, A. Mengos, X.B. Chang, A. Aleksandrov, J.R. Riordan, Differential interactions of nucleotides at the two nucleotide binding domains of the cystic fibrosis transmembrane conductance regulator, J. Biol. Chem. 276 (2001) 12918–12923.
[38] L. Aleksandrov, A.A. Aleksandrov, X.B. Chang, J.R. Riordan, The first nucleotide binding domain of cystic fibrosis transmembrane conductance regulator is a site of stable nucleotide interaction, whereas the second is a site of rapid turnover, J. Biol. Chem. 277 (2002) 15419–15425.
[39] L.W. Hung, I.X. Wang, K. Nikaido, P.Q. Liu, G.F. Ames, S.H. Kim, Crystal structure of the ATP-binding subunit of an ABC transporter, Nature 396 (1998) 703–707.
[40] P.C. Smith, N. Karpowich, L. Millen, J.E. Moody, J. Rosen, P.J. Thomas, J.F. Hunt, ATP binding to the motor domain from an ABC transporter drives formation of a nucleotide sandwich dimer, Mol. Cell 10 (2002) 139–149.
[41] J.E. Moody, L. Millen, D. Binns, J.F. Hunt, P.J. Thomas, Cooperative, ATP-dependent association of the nucleotide binding cassettes during the catalytic cycle of ATP-binding cassette transporters, J. Biol. Chem. 277 (2002) 21111–21114.
[42] I.L. Urbatsch, M. Julien, I. Carrier, M.E. Rousseau, R. Cayrol, P. Gros, Mutational analysis of conserved carboxylate residues in the nucleotide binding sites of P-glycoprotein, Biochemistry 39 (2000) 14138–14149.
[43] L.F. Payen, M. Gao, C.J. Westlake, S.P. Cole, R.G. Deeley, Role of carboxylate residues adjacent to the conserved core Walker B motifs in the catalytic cycle of multidrug resistance protein 1 (ABCC1), J. Biol. Chem. 278 (2003) 38537–38547.
[44] X.B. Chang, Y.X. Hou, J.R. Riordan, ATPase activity of purified multidrug resistance-associated protein [published erratum appears in J. Biol. Chem. 1998 Mar 27;273(13):7782], J. Biol. Chem. 272 (1997) 30962–30968.
[45] M. Kozak, Point mutations define a sequence flanking the AUG initiator codon that modulates translation by eukaryotic ribosomes, Cell 44 (1986) 283–292.
[46] I. Leier, G. Jedlitschky, U. Buchholz, D. Keppler, Characterization of the ATP-dependent leukotriene C4 export carrier in mastocytoma cells, Eur. J. Biochem. 220 (1994) 599–606.
[47] D.W. Loe, K.C. Almquist, R.G. Deeley, S.P. Cole, Multidrug resistance protein (MRP)-mediated transport of leukotriene C4 and chemotherapeutic agents in membrane vesicles. Demonstration of glutathione-dependent vincristine transport, J. Biol. Chem. 271 (1996) 9675–9682.
[48] L. Manciu, X.B. Chang, J.R. Riordan, J.M. Ruysschaert, Multidrug resistance protein MRP1 reconstituted into lipid vesicles: secondary structure and nucleotide-induced tertiary structure changes, Biochemistry 39 (2000) 13026–13033.
[49] L. Manciu, X.B. Chang, J.R. Riordan, F. Buyse, J.M. Ruysschaert, Nucleotide-induced conformational changes in the human multidrug resistance protein MRP1 are related to the capacity of chemotherapeutic drugs to accumulate or not in resistant cells, FEBS Lett. 493 (2001) 31–35.
[50] L. Manciu, X.B. Chang, F. Buyse, Y.X. Hou, A. Gustot, J.R. Riordan, J.M. Ruysschaert, Intermediate structural states involved in MRP1-mediated drug transport. Role of glutathione, J. Biol. Chem. 278 (2003) 3347–3356.
[51] Y.X. Hou, J.R. Riordan, X.B. Chang, ATP binding, not hydrolysis, at the first nucleotide-binding domain of multidrug resistance-associated protein MRP1 enhances ADP.Vi trapping at the second domain, J. Biol. Chem. 278 (2003) 3599–3605.
[52] Q. Zhao, X.B. Chang, Mutation of the aromatic amino acid interacting with adenine moiety of ATP to a polar residue alters the properties of multidrug resistance protein 1, J. Biol. Chem. 279 (2004) 48505–48512.